

## Article

# High-Temperature Dielectric and Microwave Absorption Property of Atmospheric Plasma Sprayed Al<sub>2</sub>O<sub>3</sub>-MoSi<sub>2</sub>-Cu Composite Coating

Cheng Gao <sup>1,2</sup>, Yangsheng Jiang <sup>2</sup>, Dayong Cai <sup>1,\*</sup>, Jinyong Xu <sup>2</sup> and Jia Ding <sup>2</sup>

<sup>1</sup> College of Materials Science and Engineering, Yanshan University, No. 438 West Hebei Avenue, Qinhuangdao 066004, China; cgao1982@126.com

<sup>2</sup> School of Mechanical and Electrical Engineering, Guilin University of Electronic Technology, No. 1 of Jinji Road, Guilin 541004, China; bobi6658@hotmail.com (Y.J.); xujinyong62@163.com (J.X.); djguet@126.com (J.D.)

\* Correspondence: cdy@ysu.edu.cn

**Abstract:** Al<sub>2</sub>O<sub>3</sub>-MoSi<sub>2</sub> coating has excellent high-temperature stability. On this basis, Al<sub>2</sub>O<sub>3</sub>-MoSi<sub>2</sub>-Cu composite high-temperature absorbing coating was prepared by atmospheric plasma spraying method. The phase transition characteristics of Al<sub>2</sub>O<sub>3</sub>-MoSi<sub>2</sub>-Cu spraying feedstock under high temperatures were analyzed by thermogravimetric test, the phase analysis of coating was performed by an in situ XRD test at different temperatures, and the microstructure of the coating was characterized by SEM. The test results of high-temperature microwave absorption performance show that, in high-temperature air atmosphere, the Cu in the coating is gradually transformed into Cu<sub>2</sub>O by oxygen atom diffusion, and the microwave absorption performance of the coating gradually increases with the increase in temperature. The 1.7 mm-thick coating at 500 °C has the best absorbing performance with a reflection loss (RL) value of −17.96 dB and an effective absorbing bandwidth (RL < −10 dB) in X-band of 2.42 GHz. The prepared Al<sub>2</sub>O<sub>3</sub>-MoSi<sub>2</sub>-Cu composite high-temperature absorbing coating takes into account the dual advantages of high-temperature stability and high-temperature absorbing properties.

**Keywords:** atmospheric plasma spraying; thermal analysis; absorbing coating; Al<sub>2</sub>O<sub>3</sub>-MoSi<sub>2</sub>-Cu



**Citation:** Gao, C.; Jiang, Y.; Cai, D.; Xu, J.; Ding, J. High-Temperature Dielectric and Microwave Absorption Property of Atmospheric Plasma Sprayed Al<sub>2</sub>O<sub>3</sub>-MoSi<sub>2</sub>-Cu Composite Coating. *Coatings* **2021**, *11*, 1029. <https://doi.org/10.3390/coatings11091029>

Academic Editor: Devis Bellucci

Received: 2 August 2021

Accepted: 25 August 2021

Published: 27 August 2021

**Publisher's Note:** MDPI stays neutral with regard to jurisdictional claims in published maps and institutional affiliations.



**Copyright:** © 2021 by the authors. Licensee MDPI, Basel, Switzerland. This article is an open access article distributed under the terms and conditions of the Creative Commons Attribution (CC BY) license (<https://creativecommons.org/licenses/by/4.0/>).

## 1. Introduction

With the rapid development of radar detection technology, absorbing materials have attracted more and more attention, especially high-temperature absorbing materials. The commonly used dielectric materials include Ti<sub>3</sub>SiC<sub>2</sub> [1], SiC<sub>f</sub> [2], and Al<sub>2</sub>O<sub>3</sub>-TiC [3], and the magnetic materials include Fe<sub>3</sub>Si [4], Cr<sub>2</sub>AlB<sub>2</sub> [5], Fe@MoS<sub>2</sub> [6], etc. The absorbing materials include SiCN(CNTs) [7] and SiCO@BN [8], and the absorbing coatings include La<sub>0.6</sub>SrFeO<sub>3-δ</sub>/MgAl<sub>2</sub>O<sub>4</sub> [9], TiC-Al<sub>2</sub>O<sub>3</sub>/Silica [10], etc. There are many technical methods for preparing absorbing materials or absorbing coatings, among which the preparation of absorbing coatings by plasma spraying has good process convenience and practicability. In this study Al<sub>2</sub>O<sub>3</sub>, MoSi<sub>2</sub>, and Cu powders were used to prepare high-temperature absorbing coating by air plasma spraying.

MoSi<sub>2</sub> is often used as spraying feedstock for plasma spraying, which has good oxidation resistance, high-temperature resistance, wear resistance, and good dielectric properties [11,12], and is widely used in high-temperature oxidation resistant materials and coatings. Al<sub>2</sub>O<sub>3</sub> has the advantages of high hardness and high melting point, which is commonly used in the production of high-temperature resistant materials; after fully mixing with MoSi<sub>2</sub>, the high-temperature stability of MoSi<sub>2</sub> can be enhanced. Yan et al. [13] prepared Mo coatings and MoSi<sub>2</sub>-Mo coatings using a plasma spraying method. The results showed that the MoSi<sub>2</sub> composition could improve the micro hardness and wear resistance of the coatings. Hou et al. [14] mixed MoSi<sub>2</sub> with different at% Al and prepared at% Al

coating on a Ni-based superalloy by means of electrothermal explosive high-speed spraying. The oxidation resistance of the coating in the air at 1100 °C was studied. The results showed that the addition of Al to MoSi<sub>2</sub> could effectively improve the oxidation resistance of the coating. Huang et al. [15] prepared Al<sub>2</sub>O<sub>3</sub>/MoSi<sub>2</sub> coating by a brushing method and found that, when the content of MoSi<sub>2</sub> was 20%, the surface of the Al<sub>2</sub>O<sub>3</sub>/MoSi<sub>2</sub> coating remained intact after 25 thermal shock cycles. The results showed that the content of MoSi<sub>2</sub> had an effect on the high-temperature resistance of Al<sub>2</sub>O<sub>3</sub>/MoSi<sub>2</sub> coating. Huo et al. [16] used a plasma spraying method and flame spraying method to spray MoSi<sub>2</sub>-Al<sub>2</sub>O<sub>3</sub> powder on the surface of 310S stainless steel. After a 1200 °C high-temperature oxidation test, the coating prepared by a flame spraying process appeared powdered and peeled off, while the quality of the coating prepared by plasma spraying process was intact.

Cu has excellent electrical conductivity and wear resistance, but the dielectric loss performance of Cu is not obvious when it is used as a wave absorbent alone. Singh et al. [17] mixed Cu with different mass fraction into SiC by ball milling and designed a double-layer absorbing coating by genetic algorithm. The minimum reflection loss of the coating with a thickness of 1.67 mm in X-band reached −32.16 dB, and the absorption bandwidth (RL < −10 dB) was 2.35 GHz. Yang et al. [18] synthesized Cu-based MOF composites through Cu<sub>2</sub>O@NPC and found that the content of Cu<sub>2</sub>O can change the dielectric constant of the coating, thus obtaining a broadband absorbing material. The absorbing bandwidth (RL < −10 dB) of the coating with a thickness of 1.85 mm can reach 7.3 GHz, and the minimum reflection loss can reach −31.1 dB at 5.6 GHz. Gao et al. [19] prepared Cu<sub>2</sub>O/MWCNT hybrid materials by precipitation method. The hybrid materials have excellent microwave absorption properties. When the coating thickness is 1.5 mm, the minimum reflection loss of the coating reaches −40.5 dB at 8.1 GHz test frequency.

In this study, Al<sub>2</sub>O<sub>3</sub>, MoSi<sub>2</sub>, and Cu powders were used to prepare high-temperature microwave absorbing coatings. Both Al<sub>2</sub>O<sub>3</sub> and MoSi<sub>2</sub> have excellent high-temperature resistance, and Cu has good electrical conductivity. However, the preparation of high-temperature absorbing coatings with high-temperature resistance by mixing Al<sub>2</sub>O<sub>3</sub>, MoSi<sub>2</sub>, and Cu is rarely studied. In this study, Cu was the coating inner and surface. Therefore, Cu can be oxidized to different degrees in a high-temperature environment of 500 °C; the Cu transforms to Cu<sub>2</sub>O in high temperatures, which will improve the absorbing performance of the coating. The high-temperature resistance of the two spray feedstocks was compared. The microstructure and phase composition of Al<sub>2</sub>O<sub>3</sub>-MoSi<sub>2</sub>-Cu coating were studied, and the process of Cu transforming into Cu<sub>2</sub>O, the key component, was analyzed at different temperatures. The polarization phenomenon of the coating with the increase in temperature further enhances the dielectric loss ability of the coating. With the continuous increase in Cu<sub>2</sub>O in the coating, the microwave absorbing performance of the coating is gradually enhanced, especially in the high-temperature environment.

## 2. Materials and Methods

This experiment uses atmospheric plasma spraying equipment (SX-80, GuangZong Sanxin Company, Guangzhou, China). The Al<sub>2</sub>O<sub>3</sub>-MoSi<sub>2</sub>-Cu coating was prepared by plasma spraying method, and the sprayed coating was cut into rectangular samples for testing dielectric properties in X-band. The oxidation reaction of spraying feedstock in air atmosphere was tested by thermal analyzer (TGA, TGA400, PerkinElmer, Waltham, MA, USA), the microstructure of the coating surface was observed by scanning electron microscopy (SEM, Quanta 450 FEG, FEI Company, Hillsboro, OR, USA), and the phase analysis of the coating was characterized by operando-XRD (XRD, D8-Advance, Bruker, Bremen, Germany, Cu-K $\alpha$  radiation). The dielectric constant of the coating between 25 and 500 °C was measured by a vector network analyzer (Agilent E8363B PNA, Santa Clara, CA, USA).

### 2.1. Preparation of Spraying Feedstock

$\text{Al}_2\text{O}_3$ ,  $\text{MoSi}_2$ , and Cu powder were evenly mixed in the experiment. The particle size of  $\text{Al}_2\text{O}_3$  powder was 30 to 60  $\mu\text{m}$ , and it was produced by Shanghai Xiangtian Nano Co., Ltd. (Shanghai, China); the shape was spherical and the surface was wavy. The particle size of  $\text{MoSi}_2$  powder was from 15 to 40  $\mu\text{m}$ , and it was produced by Shanghai Naio Nano Co., Ltd. (Shanghai, China). The shape of  $\text{MoSi}_2$  powder particles was irregular flocculent and there were small holes on the surface. The particle size of Cu ranged from 10 to 30  $\mu\text{m}$ , and it was produced by Shanghai Naio Nano Co., Ltd. (Shanghai, China); the shape was ellipsoidal and the surface was smooth.  $\text{Al}_2\text{O}_3$  powder,  $\text{MoSi}_2$  powder, and Cu powder were mixed by planetary ball mill and ground at 300 r/min for 4 h. At the same time, alcohol was added in the process of ball milling to make three kinds of mixed particles, stirred evenly. The  $\text{Al}_2\text{O}_3$ - $\text{MoSi}_2$ -Cu mixed powder (70 wt%  $\text{Al}_2\text{O}_3$  + 15 wt%  $\text{MoSi}_2$  + 15 wt% Cu) obtained by ball milling was dried by a dryer and ground by bowl; the prepared spray feedstock had excellent fluidity. SEM micrographs of  $\text{Al}_2\text{O}_3$ - $\text{MoSi}_2$ -Cu mixed powders are shown in Figure 1.

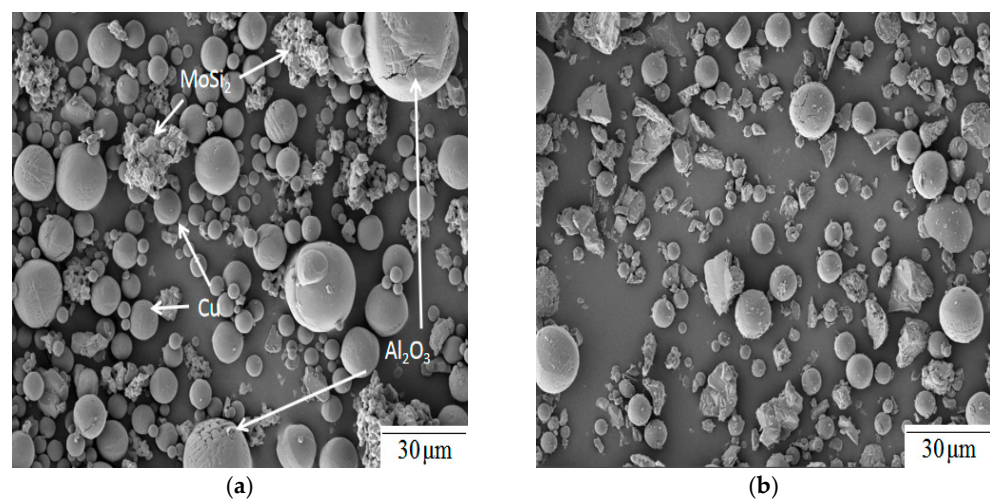


**Figure 1.** SEM micrographs of  $\text{Al}_2\text{O}_3$ - $\text{MoSi}_2$ -Cu mix powders: (a) the original powders; (b) ball milling for 4 h after spray feedstock.

### 2.2. Plasma Spraying Experiment

The  $\text{Al}_2\text{O}_3$ - $\text{MoSi}_2$ -Cu coating was prepared by plasma spraying method. The substrate needs to be pretreated, including sand blasting and oil removal; these two processes can make the substrate reach the surface conditions required by plasma spraying on the substrate. Finally,  $\text{Al}_2\text{O}_3$ - $\text{MoSi}_2$ -Cu mixed powder is sprayed on the surface of the substrate. In the process of atmospheric plasma spraying, the main gas is Ar, and the secondary gas is  $\text{H}_2$ . Ar as inert gas has good protection for spraying feedstock.  $\text{H}_2$  can be used as a secondary gas to reduce gas, so adding  $\text{H}_2$  can effectively prevent Cu and  $\text{MoSi}_2$  from being oxidized. The plasma spraying parameters are shown in Table 1.

**Table 1.** Atmosphere plasma spraying parameter.

Parameters	Value
Arc Current (A)	400
Arc Voltage (V)	30
Primary gas (Ar) flow rate (L/h)	1800
Secondary gas ( $\text{H}_2$ ) rate (L/h)	10
Spray distance (mm)	85
Powder carrier gas (Ar) flow rate (L/h)	200
Powder feed rate (g/min)	20

### 2.3. Micromorphology of Coating

SEM micrographs of  $\text{Al}_2\text{O}_3$ - $\text{MoSi}_2$ -Cu mixed coatings are shown in Figure 2.  $\text{Al}_2\text{O}_3$ - $\text{MoSi}_2$ -Cu powder, by plasma spraying process, formed a coating on the surface of the substrate. It can be seen from Figure 2a that there are micro holes on the surface of the coating, which are unavoidable during plasma spraying. Additionally, the existence of reasonable porosity can enhance the heat dissipation capacity of the coating. From Figure 2b, it can be found that there are  $\text{Al}_2\text{O}_3$ ,  $\text{MoSi}_2$ , and Cu particles on the irregular surface of the coating, and the three particles are uniformly distributed on the surface of the coating, forming an  $\text{Al}_2\text{O}_3$ - $\text{MoSi}_2$ -Cu mixed coating.

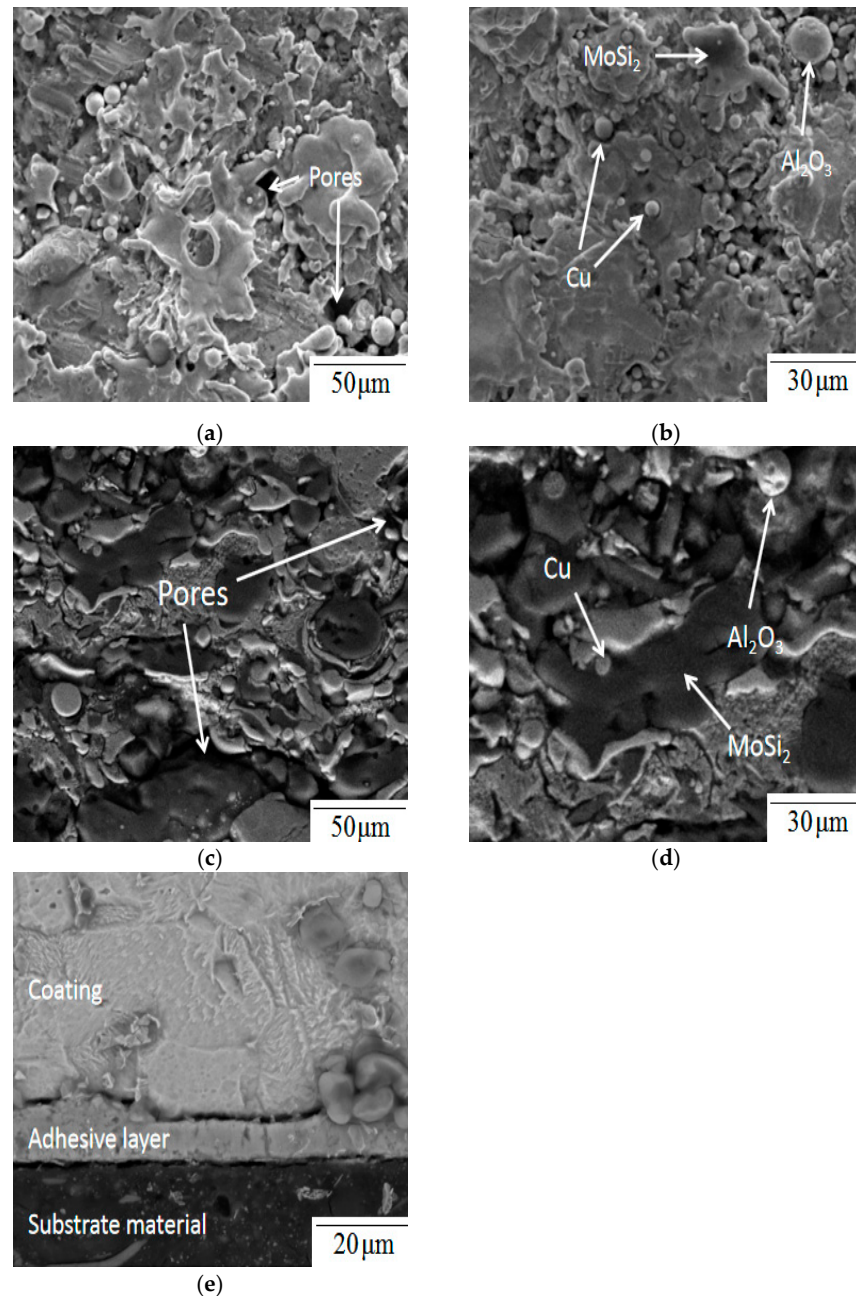


**Figure 2.** SEM micrographs of the  $\text{Al}_2\text{O}_3$ - $\text{MoSi}_2$ -Cu coating: (a) some pores exist in  $\text{Al}_2\text{O}_3$ - $\text{MoSi}_2$ -Cu coating surface; (b) distribution of different particles on coating's surface; (c) fracture surface SEM micrograph of the  $\text{Al}_2\text{O}_3$ - $\text{MoSi}_2$ -Cu coating; (d) distribution of different particles in the coating's fracture surface; (e) fracture surface SEM micrograph of substrate material and coating.

## 2.4. Properties of the Coating

The microwave absorbing properties of the Al<sub>2</sub>O<sub>3</sub>-MoSi<sub>2</sub>-Cu mixed coating at high temperatures were tested by a Agilent E8363B PNA series vector network analyzer. The waveguide method is used in the X-band test, and the coating needs to be cut into a standard size of 22.9 × 10.2 × 2 mm<sup>3</sup>. The coating needs to be kept warm for two hours before testing, and then the coating that meets the test specifications is tested by a vector network analyzer. The test temperature is 25–500 °C, and the test frequency is 8.2–12.4 GHz (X-band). The dielectric constant of Al<sub>2</sub>O<sub>3</sub>-MoSi<sub>2</sub>-Cu mixed coating can be expressed as  $\epsilon_r = \epsilon' - j\epsilon''$ .

The reflection loss of Al<sub>2</sub>O<sub>3</sub>-MoSi<sub>2</sub>-Cu mixed coating can be calculated by Formula (1) [20] and Formula (2) [21].

$$R = 20 \lg \left| \frac{Z_{in} - 1}{Z_{in} + 1} \right| \quad (1)$$

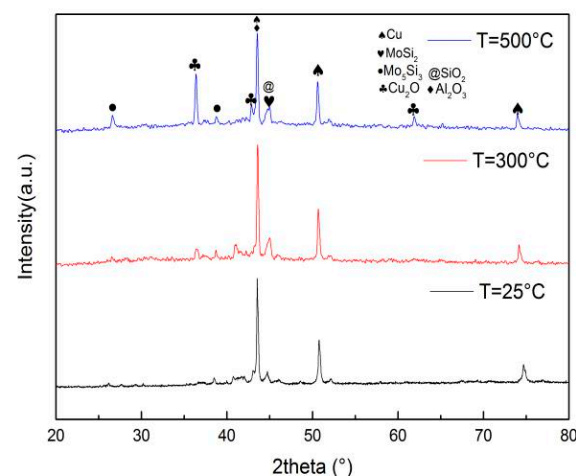
$$Z_{in} = \sqrt{\frac{\mu_r}{\epsilon_r}} \tanh \left( j \frac{2\pi f d}{c} \sqrt{\mu_r \epsilon_r} \right) \quad (2)$$

In the formula,  $Z_{in}$  is the input impedance,  $f$  is the frequency of the electromagnetic wave,  $d$  is the thickness of the coating, and  $c$  is the speed of light in a vacuum. Because Al<sub>2</sub>O<sub>3</sub>-MoSi<sub>2</sub>-Cu mixed coating is dielectric material at high temperature, the value of  $\mu_r$  is 1.

## 3. Results and Discussion

### 3.1. Phase Analysis of the Coating

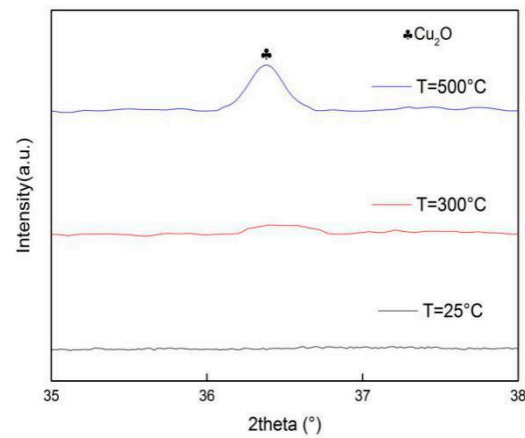
The transformation process of the Al<sub>2</sub>O<sub>3</sub>-MoSi<sub>2</sub>-Cu coating from Cu to Cu<sub>2</sub>O at different temperatures was analyzed by XRD, and the compounds produced by the Al<sub>2</sub>O<sub>3</sub>-MoSi<sub>2</sub>-Cu coating at different temperatures were determined. Figure 3 shows the XRD patterns at different temperatures, and the range of  $2\theta$  is 20–80°. It can be seen from Figure 3 that the diffraction peak of Cu<sub>2</sub>O is not obvious at room temperature (25 °C), and only a weak peak appears at 42°. This is because a small quantity of Cu<sub>2</sub>O is produced by high-temperature oxidation of Cu during plasma spraying. With the temperature reaching 500 °C, the characteristic peak of Cu<sub>2</sub>O becomes sharp at 36° and gradually highlights at approximately 61°, indicating that Cu gradually transforms into Cu<sub>2</sub>O with the increase in temperature.



**Figure 3.** XRD patterns of Al<sub>2</sub>O<sub>3</sub>-MoSi<sub>2</sub>-Cu coatings at different temperatures.

Figure 4 is a locally enlarged XRD pattern in Figure 3, as shown in Figure 3, when the temperature rises from 25 to 500 °C. No characteristic peak appears at 25 °C; when the temperature rises to 300 °C, a single peak gradually bulges and becomes sharp at 500 °C. This shows that Al<sub>2</sub>O<sub>3</sub>-MoSi<sub>2</sub>-Cu coating will produce new compounds with the increase

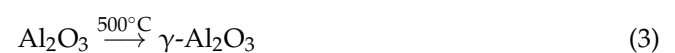
in temperature of air atmosphere. Through the comparison of three temperatures, it can clearly be observed that Cu in the coating will gradually transform into  $\text{Cu}_2\text{O}$ .



**Figure 4.** Figure 3 locally enlarged graphs in the range of  $2\theta$  from  $35^\circ$  to  $38^\circ$ .

### 3.2. Thermal Analysis

Thermogravimetric analysis of  $\text{Al}_2\text{O}_3$ - $\text{MoSi}_2$  powder and  $\text{Al}_2\text{O}_3$ - $\text{MoSi}_2$ -Cu powder was performed by thermal analyzer, with a test temperature from room temperature ( $25^\circ\text{C}$ ) to  $1000^\circ\text{C}$  and a heating rate of 10 degrees Celsius per minute.  $\text{MoSi}_2$  and  $\text{Al}_2\text{O}_3$  are selected because  $\text{MoSi}_2$  has good high-temperature resistance and is commonly used in high-temperature structures in the aerospace field. However, with the increase in temperature, the “peeling” phenomenon [22] usually occurs at 400 to  $600^\circ\text{C}$ , and the appropriate mixing of  $\text{Al}_2\text{O}_3$  in  $\text{MoSi}_2$  can effectively prevent the  $\text{MoSi}_2$  occurrence of pulverizing in the coating surface. In Figure 5, the black curves show the weight change trend of  $\text{Al}_2\text{O}_3$ - $\text{MoSi}_2$  powder during heating. It can be seen that  $\text{Al}_2\text{O}_3$ - $\text{MoSi}_2$  powder increases with temperature, and the weight of powder remains stable below  $500^\circ\text{C}$ . When  $\text{Al}_2\text{O}_3$ - $\text{MoSi}_2$  powder rises from  $500$  to  $800^\circ\text{C}$ , the mass of powder increases by 1.36%. When the temperature of  $\text{Al}_2\text{O}_3$ - $\text{MoSi}_2$  powder changes from  $800$  to  $1000^\circ\text{C}$ , it goes through a process of decrease and increase, and, finally, remains at approximately 100%. It can be seen from the thermogravimetric curve of  $\text{Al}_2\text{O}_3$ - $\text{MoSi}_2$  powder that there is no weight decrease phenomenon in the  $\text{Al}_2\text{O}_3$ - $\text{MoSi}_2$  powder. The quality of the  $\text{Al}_2\text{O}_3$ - $\text{MoSi}_2$  powder did not drop sharply, but remained stable. This shows that the content of  $\text{Al}_2\text{O}_3$ - $\text{MoSi}_2$  powder is reasonable and has high-temperature stability. The red curve in Figure 5 is the weight change trend of  $\text{Al}_2\text{O}_3$ - $\text{MoSi}_2$ -Cu powder during the heating process. It can be found that, due to the addition of Cu, when  $\text{Al}_2\text{O}_3$ - $\text{MoSi}_2$ -Cu powder is heated from  $400$  to  $1000^\circ\text{C}$ , the mass of  $\text{Al}_2\text{O}_3$ - $\text{MoSi}_2$ -Cu powder increases gradually. When the temperature reaches  $1000^\circ\text{C}$ , the mass increases by 10%, relative to the original weight, because different compounds result from oxidation with the increase in temperature of air atmosphere, which increase the quality of  $\text{Al}_2\text{O}_3$ - $\text{MoSi}_2$ -Cu powder.  $\text{Al}_2\text{O}_3$  phase transformation occurs in different temperature environments. According to the report,  $\text{Al}_2\text{O}_3$  was transformed to  $\gamma$ - $\text{Al}_2\text{O}_3$  [23] at a temperature of  $500^\circ\text{C}$ ; when the temperature reaches  $900^\circ\text{C}$ ,  $\gamma$ - $\text{Al}_2\text{O}_3$  will continue to transform in to  $\theta$ - $\text{Al}_2\text{O}_3$  [23].  $\text{MoSi}_2$  will be transformed to  $\text{Mo}_5\text{Si}_3$  in a high-temperature environment, and  $\text{SiO}_2$  will be formed [24]. Cu was oxidized to  $\text{Cu}_2\text{O}$ , and  $\text{Cu}_2\text{O}$  further oxidized to  $\text{CuO}$  in a high-temperature environment with sufficient air [25]. Chemical reactions and phase transitions of  $\text{Al}_2\text{O}_3$ - $\text{MoSi}_2$  and  $\text{Al}_2\text{O}_3$ - $\text{MoSi}_2$ -Cu powders at different temperatures can be expressed by chemical Formulaes (3)–(7).



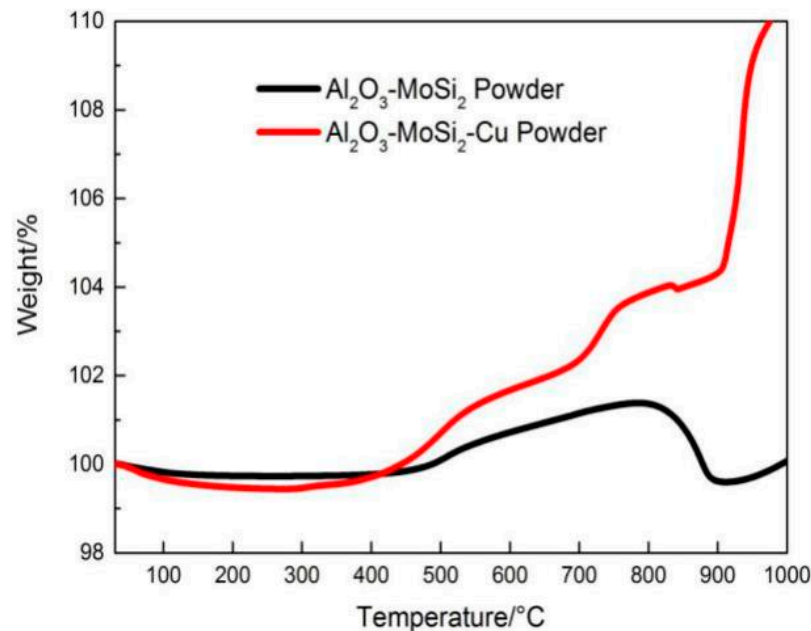


**Figure 5.** Thermogravimetric curve of Al<sub>2</sub>O<sub>3</sub>-MoSi<sub>2</sub> powder and Al<sub>2</sub>O<sub>3</sub>-MoSi<sub>2</sub>-Cu powder.

The thermogravimetric curves show that Al<sub>2</sub>O<sub>3</sub>-MoSi<sub>2</sub> powder can increase the high-temperature oxidation resistance of the material. The CuO [26] and Cu<sub>2</sub>O formed by Cu oxidation at high temperature can improve the microwave absorption performance of the material.

### 3.3. Dielectric Properties of the Coating

The dielectric properties of the coating at room temperature (25 °C) to 500 °C were tested; Figure 6a shows the change of the real part of dielectric constant of Al<sub>2</sub>O<sub>3</sub>-MoSi<sub>2</sub>-Cu coating with increasing microwave frequency at different temperatures. In the 8.5 GHz microwave frequency environment at 500 °C, the dielectric constant of the coating is 25.29. When the frequency increases to 12 GHz, the dielectric constant is 20.05. Figure 6b shows the change in the imaginary part of the dielectric constant of the Al<sub>2</sub>O<sub>3</sub>-MoSi<sub>2</sub>-Cu coating with the increase in microwave frequency at different temperatures: at 500 °C, the imaginary part of the dielectric constant is 4.43 at 8.5 GHz microwave frequency and 5.34 at 12 GHz. Figure 6c shows that the tanδ of the Al<sub>2</sub>O<sub>3</sub>-MoSi<sub>2</sub>-Cu coating increases from 0.181 at 8.5 GHz to 0.271 at 12 GHz at 500 °C. It can be seen that the loss ability of the Al<sub>2</sub>O<sub>3</sub>-MoSi<sub>2</sub>-Cu coating increases with the increase in environment temperature. The dielectric constant of the coating increases with the increase in temperature, but the dielectric constant decreases with the increase in frequency at different temperatures; this phenomenon—that the dielectric constant decreases with the increase in frequency—fully conforms to the dispersion effect [27]. Figure 6e is the permittivity of the Al<sub>2</sub>O<sub>3</sub>-MoSi<sub>2</sub>-Cu<sub>2</sub>O coating by the same process. The ε' is 8.51 and the ε'' is 1.66 in the 8.5 GHz microwave frequency. The frequency increases to 12 GHz, ε' is 8.27, and ε'' is 2.12. The Al<sub>2</sub>O<sub>3</sub>-MoSi<sub>2</sub>-Cu<sub>2</sub>O coating is not affected by temperature, so the permittivity changes little.

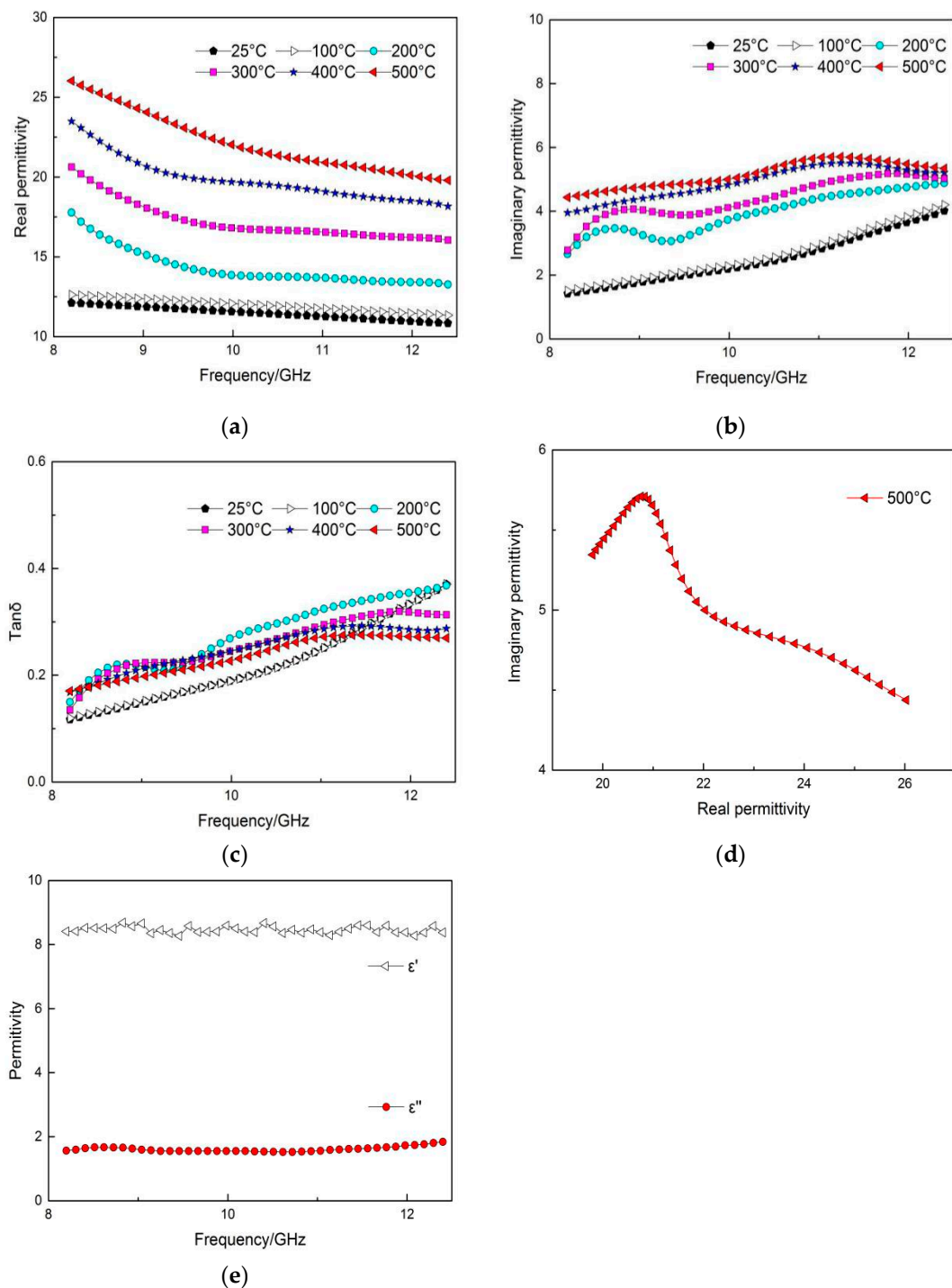


**Figure 6.** Dielectric properties of Al<sub>2</sub>O<sub>3</sub>-MoSi<sub>2</sub>-Cu composite coating: (a)  $\epsilon'$  of Al<sub>2</sub>O<sub>3</sub>-MoSi<sub>2</sub>-Cu composite coating; (b)  $\epsilon''$  of Al<sub>2</sub>O<sub>3</sub>-MoSi<sub>2</sub>-Cu composite coating; (c) Tan $\delta$  of Al<sub>2</sub>O<sub>3</sub>-MoSi<sub>2</sub>-Cu composite coating; (d) the Cole–Cole plot of Al<sub>2</sub>O<sub>3</sub>-MoSi<sub>2</sub>-Cu composite coating with the fitting date in 500 °C; (e) permittivity of Al<sub>2</sub>O<sub>3</sub>-MoSi<sub>2</sub>-Cu<sub>2</sub>O composite coating at room temperature (25 °C).

The  $\epsilon'$  and  $\epsilon''$  of Al<sub>2</sub>O<sub>3</sub>-MoSi<sub>2</sub>-Cu<sub>2</sub>O composite coating can be expressed as Formulaes (8) and (9) according to the Debye model [28].

$$\epsilon' = \epsilon_{\infty} + \frac{\epsilon_s - \epsilon_{\infty}}{1 + \omega^2\tau^2} \tag{8}$$

$$\varepsilon'' = \frac{(\varepsilon_s - \varepsilon_\infty)\omega\tau}{1 + \omega^2\tau^2} \quad (9)$$

In the equation,  $\varepsilon_s$  is static dielectric constant and  $\varepsilon_\infty$  is optical frequency dielectric constant. The  $\text{Al}_2\text{O}_3$ - $\text{MoSi}_2$ -Cu coating permittivity change in real part and imaginary part at high temperatures can be deduced by Formulas (10) and (11) [29,30].

$$\varepsilon' = \varepsilon_\infty + \frac{\varepsilon_s - \varepsilon_\infty}{1 + \omega^2\tau(T)^2} \quad (10)$$

$$\varepsilon'' = \varepsilon_\infty + \frac{(\varepsilon_s - \varepsilon_\infty)\omega\tau(T)}{1 + \omega^2[\omega\tau(T)]^2} + \frac{\sigma(T)}{\omega\varepsilon_0} \quad (11)$$

In the equation,  $\tau(T)$  is polarization relaxation time influenced by temperature,  $\varepsilon_0$  is the vacuum dielectric constant, and  $\sigma(T)$  is the conductivity affected by temperature

The change in  $\varepsilon'$  and  $\varepsilon''$  can be obtained by Formulae (10) and (11). This is because the external electric field of the coating changes with the temperature. The change of polar molecules inside the coating cannot keep up with the drastic change in external electric field caused by temperature. Figure 6d is the Cole–Cole fitting plot of  $\text{Al}_2\text{O}_3$ - $\text{MoSi}_2$ -Cu coating at 500 °C; it can be seen that there are two incomplete and irregular semicircles rather than a complete semicircle in the figure, indicating that the coating has not only Debye relaxation but also other relaxation [31] mechanisms at high temperatures. The irregular semicircles show that the  $\text{Al}_2\text{O}_3$ - $\text{MoSi}_2$ -Cu coating has two losses at 500 °C.  $\text{Al}_2\text{O}_3$ - $\text{MoSi}_2$ -Cu coating is made of an electrical material and is dominated by dielectric loss. The  $\varepsilon'$  and  $\varepsilon''$  of the coating increase with the increase in temperature. A conductive network is formed by  $\text{Al}_2\text{O}_3$  and  $\text{MoSi}_2$  in the coating [12]. With the increase in temperature, Cu gradually transforms into  $\text{Cu}_2\text{O}$ , and the conductive network formed together with  $\text{Al}_2\text{O}_3$  and  $\text{MoSi}_2$  enhances the conductivity loss of the coating. It can be seen that  $\text{Al}_2\text{O}_3$ - $\text{MoSi}_2$ -Cu coating has significant dielectric properties at high temperature.

### 3.4. Absorbing Performance of the Coating

The absorbing properties of the coating are shown in Figure 7. Figure 7b shows that the absorption peak of  $\text{Al}_2\text{O}_3$ - $\text{MoSi}_2$ -Cu coating with 1.5 mm thickness is approximately 11 GHz. The absorption performance of the coating is not obvious at 25 °C. The minimum reflection loss is −3.09 dB at 11.4 GHz and −16.07 dB at 500 °C. The coating has the best absorbing property at 500 °C; it shows that  $\text{Al}_2\text{O}_3$ - $\text{MoSi}_2$ -Cu coating has good high-temperature absorbing properties. With the increase in temperature, the dielectric constant of the coating increases, and the absorbing bandwidth of the coating moves from high frequency to low frequency. This law conforms to Formula (12) [32].

$$f_m = \frac{c}{4d\sqrt{\varepsilon_r\mu_r}} \quad (12)$$

In the equation,  $d$  is the thickness of the coating, and  $c$  is the speed of light in vacuum. Microwave absorbing properties of  $\text{Al}_2\text{O}_3$ - $\text{MoSi}_2$ -Cu coatings improved significantly from room temperature (25 °C) to 500 °C, mainly due to the transformation of Cu on the coating surface into  $\text{Cu}_2\text{O}$  in air atmosphere;  $\text{Cu}_2\text{O}$  can effectively improve the absorbing properties of materials [33]. According to Figure 3—the XRD pattern results of the coating—the characteristic peak of  $\text{Cu}_2\text{O}$  became obvious at 500 °C, indicating that  $\text{Cu}_2\text{O}$  was generated. It can be seen from Figure 2 SEM micrographs that there are different sizes of pores in the coating; as the temperature rises, the air reacts with Cu on the coating surface and enters the coating from the pores to react with Cu. The reason for the formation of  $\text{Cu}_2\text{O}$  is that Cu is first transformed into  $\text{Cu}_2\text{O}$  due to insufficient oxygen during heating. There are also peaks of Cu. It is indicated that a  $\text{Cu}_2\text{O}/\text{Cu}$  mixture exists in the coating, which is due to the fact that Cu in the coating cannot react completely with air during heating in air. Comparing Figure 6a,b,e, it can be seen that, with the temperature rises, the coating surface is the site of the oxidation reaction, in the coating inner where lattice

vibration occurs; as the temperature increases, the lattice vibrates with greater intensity. At the same time, high temperature causes a change in conductivity. These three reasons together lead to the dielectric constant change in the coating at high temperatures. Cu has strong conductivity, but the absorbing property of the composite coating is not obvious at room temperature, according to Figure 7c. The coating thickness is 1.7 mm, and the minimum reflection loss at 25 °C is only  $-4.89$  dB. The minimum reflection loss decreases to  $-17.96$  dB at 500 °C. Because Cu is transformed into  $\text{Cu}_2\text{O}$ , the conductive network is formed with  $\text{Al}_2\text{O}_3\text{-MoSi}_2$ , which enhances the absorbing loss performance of the coating.

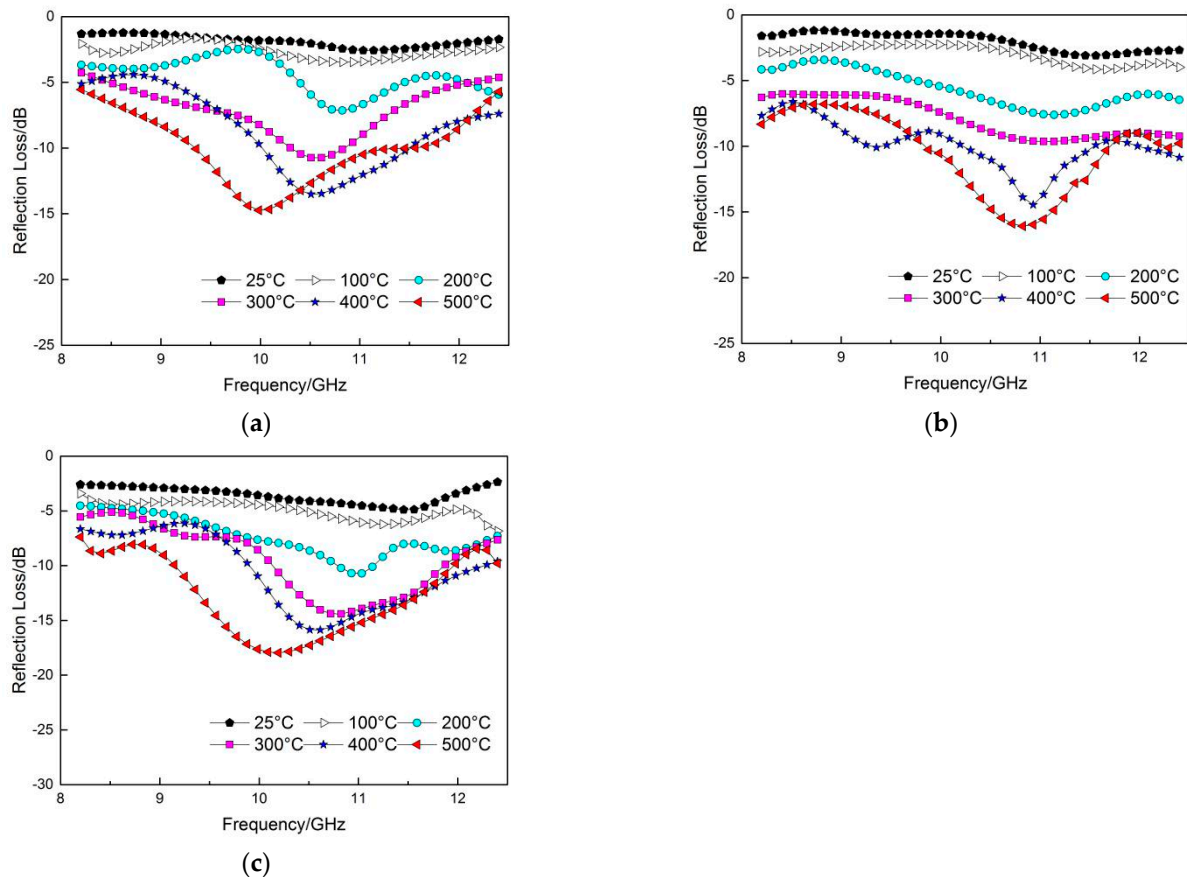


Figure 7. Reflection loss of the  $\text{Al}_2\text{O}_3\text{-MoSi}_2\text{-Cu}$  composite coatings: (a)  $d = 1.3$ ; (b)  $d = 1.5$ ; (c)  $d = 1.7$ .

The results show that the  $\text{Al}_2\text{O}_3\text{-MoSi}_2\text{-Cu}$  microwave absorbing coating has good high-temperature resistance and microwave absorption performance at 500 °C.

#### 4. Conclusions

The results show that the  $\text{Al}_2\text{O}_3\text{-MoSi}_2\text{-Cu}$  coating has good microwave absorption properties at 500 °C, and the microwave absorption performance of the coating increases with the increase in temperature. Thermogravimetric analysis assisted to verify the rationality of spray feedstock match ratio and the stability of the coating in a high-temperature environment. The phase composition of the coating and the changes in the compounds at different temperatures were studied using an in situ XRD test. Finally, the dielectric properties and microwave absorbing properties of a 1.7 mm-thick coating in the range of 25 °C–500 °C were tested by a vector network analyzer. The existence of  $\text{Cu}/\text{Cu}_2\text{O}$  mixture in the coating enhances the conductivity loss of the coating. At high temperatures,  $\text{Cu}_2\text{O}$  and  $\text{Al}_2\text{O}_3\text{-MoSi}_2$  form a conductive network, which enhances the microwave absorbing properties of the coating and has good microwave absorbing properties in X-band.

**Author Contributions:** Conceptualization, C.G. and Y.J.; methodology, C.G.; formal analysis, Y.J.; investigation, C.G.; data curation, J.D.; writing—original draft preparation, C.G. and Y.J.; writing—review and editing, D.C.; visualization, Y.J.; supervision, D.C.; project administration, J.X.; funding acquisition, J.X. All authors have read and agreed to the published version of the manuscript.

**Funding:** Guangxi S & T Program (No.AD18126024).

**Institutional Review Board Statement:** Not applicable.

**Informed Consent Statement:** Not applicable.

**Data Availability Statement:** Data are included in this article.

**Conflicts of Interest:** The authors declare no conflict of interest.

## References

1. Su, J.; Zhou, W.; Liu, Y.; Qing, Y.; Luo, F.; Zhu, D. High-Temperature Dielectric and Microwave Absorption Property of Plasma Sprayed  $\text{Ti}_3\text{SiC}_2$ /Cordierite Coatings. *J. Mater. Sci. Mater. Electron.* **2016**, *27*, 2460–2466. [[CrossRef](#)]
2. Zhou, Q.; Yin, X.; Ye, F.; Tang, Z.; Mo, R.; Cheng, L. High Temperature Electromagnetic Wave Absorption Properties of  $\text{SiCf}/\text{Si}_3\text{N}_4$  Composite Induced by Different SiC Fibers. *Ceram. Int.* **2019**, *45*, 6514–6522. [[CrossRef](#)]
3. Shao, T.; Ma, H.; Wang, J.; Feng, M.; Yan, M.; Wang, J.; Yang, Z.; Zhou, Q.; Luo, H.; Qu, S. High Temperature Absorbing Coatings with Excellent Performance Combined  $\text{Al}_2\text{O}_3$  and TiC Material. *J. Eur. Ceram. Soc.* **2020**, *40*, 2013–2019. [[CrossRef](#)]
4. Hou, Y.; Xiao, B.; Sun, Z.; Yang, W.; Wu, S.; Qi, S.; Wen, G.; Huang, X. High Temperature Anti-Oxidative and Tunable Wave Absorbing  $\text{SiC}/\text{Fe}_3\text{Si}/\text{CNTs}$  Composite Ceramic Derived from a Novel Polysilylacetylene. *Ceram. Int.* **2019**, *45*, 16369–16379. [[CrossRef](#)]
5. Zhang, H.; Zhao, B.; Xiang, H.; Dai, F.; Zhang, Z.; Zhou, Y. Electromagnetic Wave Absorbing Properties of  $\text{Cr}_2\text{AlB}_2$  Powders and the Effect of High-temperature Oxidation. *J. Am. Ceram. Soc.* **2021**, *104*, 2213–2224. [[CrossRef](#)]
6. Pan, J.; Sun, X.; Wang, T.; Zhu, Z.; He, Y.; Xia, W.; He, J. Porous Coin-like  $\text{Fe}@\text{MoSi}_2$  Composite with Optimized Impedance Matching for Efficient Microwave Absorption. *Appl. Surf. Sci.* **2018**, *457*, 271–279. [[CrossRef](#)]
7. Wang, S.; Gong, H.; Zhang, Y.; Ashfaq, M.Z. Microwave Absorption Properties of Polymer-Derived SiCN (CNTs) Composite Ceramics. *Ceram. Int.* **2021**, *47*, 1294–1302. [[CrossRef](#)]
8. Hou, Y.; Yang, W.; Zhong, C.; Wu, S.; Wu, Y.; Liu, F.; Huang, X.; Wen, G. Thermostable  $\text{SiCO}@\text{BN}$  Sheets with Enhanced Electromagnetic Wave Absorption. *Chem. Eng. J.* **2019**, *378*, 122239. [[CrossRef](#)]
9. Jia, H.; Zhou, W.; Nan, H.; Qing, Y.; Luo, F.; Zhu, D. High Temperature Microwave Absorbing Properties of Plasma Sprayed  $\text{La}_{0.6}\text{Sr}_{0.4}\text{FeO}_{3-\delta}/\text{MgAl}_2\text{O}_4$  Composite Ceramic Coatings. *Ceram. Int.* **2020**, *46*, 6168–6173. [[CrossRef](#)]
10. Wang, Y.; Luo, F.; Zhou, W.; Zhu, D. Dielectric and Microwave Absorption Properties of  $\text{TiC}-\text{Al}_2\text{O}_3/\text{Silica}$  Coatings at High Temperature. *J. Electron. Mater.* **2017**, *46*, 5225–5231. [[CrossRef](#)]
11. Zhang, Y.; Li, Y.; Bai, C. Microstructure and Oxidation Behavior of Si–MoSi<sub>2</sub> Functionally Graded Coating on Mo Substrate. *Ceram. Int.* **2017**, *43*, 6250–6256. [[CrossRef](#)]
12. Wu, Z.; Zhou, W.; Luo, F.; Zhu, D. Effect of MoSi<sub>2</sub> Content on Dielectric and Mechanical Properties of MoSi<sub>2</sub>/Al<sub>2</sub>O<sub>3</sub> Composite Coatings. *Trans. Nonferrous Met. Soc. China* **2012**, *22*, 111–116. [[CrossRef](#)]
13. Yan, J.; He, Z.; Wang, Y.; Qiu, J.; Wang, Y. Microstructure and Wear Resistance of Plasma-Sprayed Molybdenum Coating Reinforced by MoSi<sub>2</sub> Particles. *J. Therm. Spray Tech.* **2016**, *25*, 1322–1329. [[CrossRef](#)]
14. Hou, S.; Liu, Z.; Liu, D.; Li, B. Effect of Alloying with Al on Oxidation Behavior of MoSi<sub>2</sub> Coatings at 1100 °C. *Surf. Coat. Technol.* **2012**, *206*, 4466–4470. [[CrossRef](#)]
15. Huang, X.; Zhang, F.; Zhao, Y.; An, X.; Yang, J. Preparation and Properties of Al<sub>2</sub>O<sub>3</sub>/MoSi<sub>2</sub> Coating on Al<sub>2</sub>O<sub>3</sub> Base Porous Insulation Materials. *Fuhe Cailiao Xuebao/Acta Mater. Compos. Sin.* **2020**, *37*, 2870–2876. [[CrossRef](#)]
16. Huo, D.; Li, W.-S.; Feng, L.; Hu, C.-X.; Hu, W. Effects of Spraying Process on Microstructure and Properties of MoSi<sub>2</sub>-Al<sub>2</sub>O<sub>3</sub> Coating. *Surf. Technol.* **2018**, *47*, 267–273. [[CrossRef](#)]
17. Singh, S.; Sinha, A.; Zunke, R.H.; Kumar, A.; Singh, D. Double Layer Microwave Absorber Based on Cu Dispersed SiC Composites. *Adv. Powder Technol.* **2018**, *29*, 2019–2026. [[CrossRef](#)]
18. Yang, H.; Zhang, X.; Xiong, Z.; Shen, Z.; Liu, C.; Xie, Y. Cu<sub>2</sub>O@nanoporous Carbon Composites Derived from Cu-Based MOFs with Ultrabroad-Bandwidth Electromagnetic Wave Absorbing Performance. *Ceram. Int.* **2021**, *47*, 2155–2164. [[CrossRef](#)]
19. Gao, S.; Xing, H.; Li, Y.; Wang, H. Synthesis of Cu<sub>2</sub>O/Multi-Walled Carbon Nanotube Hybrid Material and Its Microwave Absorption Performance. *Res. Chem. Intermed.* **2018**, *44*, 3425–3435. [[CrossRef](#)]
20. Bi, S.; Su, X.; Li, J.; Hou, G.; Liu, Z.; Zhong, C.; Hou, Z. High-Temperature Dielectric Properties and Microwave Absorption Abilities of Bi<sub>1-x</sub>Mg<sub>x</sub>FeO<sub>3</sub> Nanoparticles. *Ceram. Int.* **2017**, *43*, 11815–11819. [[CrossRef](#)]
21. Sun, Y.; Sun, Y. Strong and Thermostable Boron-Containing Phenolic Resin-Derived Carbon Modified Three-Dimensional Needled Carbon Fiber Reinforced Silicon Oxycarbide Composites with Tunable High-Performance Microwave Absorption Properties. *Appl. Sci.* **2020**, *10*, 1924. [[CrossRef](#)]
22. Yakoboylu, G.A.; Yumak, T.; Sabolsky, K.; Sabolsky, E.M. Effect of High Temperature Preoxidation Treatment on the Oxidation Behavior of MoSi<sub>2</sub> and WSi<sub>2</sub>-Al<sub>2</sub>O<sub>3</sub> Composites. *J. Alloys Compd.* **2020**, *816*, 152499. [[CrossRef](#)]

23. Taghi-Ramezani, S.; Valefi, Z.; Mirjani, M.; Ghasemi, R. The Influence of Pyrolysing Al<sub>2</sub>O<sub>3</sub> Precursor on the High Temperature Properties of the YSZ-Al<sub>2</sub>O<sub>3</sub> Composite Coating. *Surf. Eng.* **2020**, 1–11. [[CrossRef](#)]
24. Cai, Z.; Liu, S.; Xiao, L.; Fang, Z.; Li, W.; Zhang, B. Oxidation Behavior and Microstructural Evolution of a Slurry Sintered Si-Mo Coating on Mo Alloy at 1650 °C. *Surf. Coat. Technol.* **2017**, 324, 182–189. [[CrossRef](#)]
25. Serrà, A.; Gómez, E.; Michler, J.; Philippe, L. Facile Cost-Effective Fabrication of Cu@Cu<sub>2</sub>O@CuO–Microalgae Photocatalyst with Enhanced Visible Light Degradation of Tetracycline. *Chem. Eng. J.* **2021**, 413, 127477. [[CrossRef](#)]
26. Ma, J.; Zhang, X.; Liu, W.; Ji, G. Direct Synthesis of MOF-Derived Nanoporous CuO/Carbon Composites for High Impedance Matching and Advanced Microwave Absorption. *J. Mater. Chem. C* **2016**, 4, 11419–11426. [[CrossRef](#)]
27. Benzerga, R.; Badard, M.; Méjean, C.; El Assal, A.; Le Paven, C.; Sharaiha, A. Carbon Fibers Loaded Composites for Microwave Absorbing Application: Effect of Fiber Length and Dispersion Process on Dielectric Properties. *J. Electron. Mater.* **2020**, 49, 2999–3008. [[CrossRef](#)]
28. Debye, P. *Polar Molecules*; The Chemical Catalogue Company: New York, NY, USA, 1929.
29. Song, W.; Cao, M.; Hou, Z.; Yuan, J.; Fang, X. High-Temperature Microwave Absorption and Evolutionary Behavior of Multiwalled Carbon Nanotube Nanocomposite. *Scr. Mater.* **2009**, 61, 201–204. [[CrossRef](#)]
30. Cao, M.-S.; Song, W.-L.; Hou, Z.-L.; Wen, B.; Yuan, J. The Effects of Temperature and Frequency on the Dielectric Properties, Electromagnetic Interference Shielding and Microwave-Absorption of Short Carbon Fiber/Silica Composites. *Carbon* **2010**, 48, 788–796. [[CrossRef](#)]
31. Grosse, C. A Program for the Fitting of Debye, Cole–Cole, Cole–Davidson, and Havriliak–Negami Dispersions to Dielectric Data. *J. Colloid Interface Sci.* **2014**, 419, 102–106. [[CrossRef](#)]
32. Gao, H.; Luo, F.; Wen, Q.; Jia, H.; Zhou, W.; Zhu, D. Enhanced High-temperature Dielectric and Microwave Absorption Properties of SiC Fiber-reinforced Oxide Matrix Composites. *J. Appl. Polym. Sci.* **2019**, 136, 47097. [[CrossRef](#)]
33. Zong, M.; Huang, Y.; Wu, H.; Zhao, Y.; Liu, P.; Wang, L. Facile Preparation of RGO/Cu<sub>2</sub>O/Cu Composite and Its Excellent Microwave Absorption Properties. *Mater. Lett.* **2013**, 109, 112–115. [[CrossRef](#)]